Biological response to wind and terrestrial nitrate in the western and southern continental shelves of the Gulf of Mexico

Javier González-Ramírez[1], Alejandro Parés-Sierra[1], and Jushiro Cepeda-Morales[2]

[1]Departamento de Oceanografía Físca, Centro de Investigación Científica y de Educación Superior de Ensenada, CICESE, Carretera Ensenada-Tijuana 3918 zona Playitas, Ensenada, Baja California, México.
[2]Centro Nayarita de Innovación y Transferencia de Tecnología, Universidad Autónoma de Nayarit, UAN, Ciudad de la Cultura Amado Nervo, Tepic, Nayarit, México.

Correspondence: Alejandro Parés-Sierra (apares@cicese.mx)

Abstract.

In Mexico, 16 rivers directly discharge into the Gulf of Mexico. The Mexican rivers and those coming from the United States generate large regions in which phytoplanktonic primary production possesses a seasonal component that is linked to these nutrient-rich freshwater inputs. In the present study, new flow and daily nutrient data were obtained for the largest

5   Mexican rivers. These data were integrated as forcing factors in a configuration of the hydrodynamic Coastal and Regional Ocean COmmunity model coupled to an N2PZD2 biogeochemical model. To correctly represent biological processes in coastal regions, a biological bottom condition was implemented in the biogeochemical model. With this condition, it was possible to represent remineralization on the continental shelf of the Gulf of Mexico. We present a 21 year simulation using two different configurations. The first included river forcing, and the second did not consider their influence. The results were

10 validated with satellite images of the surface concentration of chlorophyll and compared with data from previous studies. The coupled model was able to realistically reproduce the seasonal dynamics of primary production in the Gulf of Mexico based on the concentration and distribution of chlorophyll, both at the surface and in the water column. Finally, the physical processes that influence the dynamics of primary production in the deep region and continental shelf of the gulf were defined. In the deep region, primary production was dominated by vertical mixing induced by the passage of cold fronts during winter

15 and mesoscale structures. On the continental shelf, such dynamics were dominated by coastal upwelling and fluvial nutrient contributions.

1   Introduction

The Gulf of Mexico (GoM) is a semi-closed sea that covers an area of $\sim 1.5 \times 10^6$ km^2. It is located between 18–30° N

20 and 82–98° W (Fig. 1) and connects with the Atlantic Ocean through the Yucatan Channel and the Straits of Florida. The general circulation of the GoM is dominated by the Loop Current, which enters the gulf through the Yucatan Channel. The

Loop Current, as its name suggests, forms an anticyclonic semi-closed loop after it enters the gulf before exiting through the Straits of Florida. Anticyclonic mesoscale eddies detach from the Loop Current and propagate westward with speeds of ~2 km per day (Elliott, 1982). Vázquez De La Cerda et al. (2005) established that a semi-permanent cyclonic eddy forced by

25 Ekman pumping associated with wind stress curl is present in the Bay of Campeche (BOC), which is located in the southern region of the Gulf of Mexico.

The advection of low salinity water and coastal upwelling are among the relevant processes associated with wind seasonality. Coastal upwelling due to Ekman transport occurs in summer and winter in the southern and northern regions of the gulf, respectively (Zavala-Hidalgo et al., 2003, 2006). During the fall and winter, low salinity waters arrive from the Mississippi

30 and Atchafalaya rivers and the Louisiana-Texas (LATEX) platform to the Tamaulipas-Veracruz (TAVE) platform. During the summer, water is advected over the continental shelf from the TAVE to LATEX region. Of the 16 rivers that flow into the GoM from Mexican territory, the Grijalva, Usumacinta, Coatzacoalcos, Papaloapan, and Panuco rivers provide the majority of the freshwater to the gulf, with a combined flow of $\sim 2.2 \times 10^6$ m^3 per year (Fig 2). This value constitutes $\sim 90\%$ of the total runoff from Mexican territory into the GoM (CONAGUA, 2014). Together with contributions from the United States, this

35 fluvial runoff promotes the formation of large regions in which the primary productivity present has a seasonal component that is strongly linked to nitrogen-rich freshwater inputs. The information available on the nutrient content and flow of these large continental fluvial inputs is either scarce or intermittent. More importantly, measurements have often been taken in the regions of the continental basins and not in the river mouths where information on net flow is needed.

To remedy this, the flow and nutrient data reported by González-Ramírez and Parés-Sierra (2019) were integrated into a

40 hydrodynamic model coupled with a biological model in this study. An analysis was carried out in the regions for which the new hydrological data were calculated to describe the principal scales of variability of primary production. Finally, the identification of extraordinary events with regard to the responses of phytoplankton based on the new daily flow rate data were evaluated in the coupled model.

2 Model configuration

2.1 Physical model

For this study, we used the Coastal and Regional Ocean COmmunity model (CROCO) v. 1.0 (Debreu et al., 2012) to simulate the physical processes of the GoM. The model domain included the entire GoM from 79.30–98.00° W and from 18.10–30.70° N. The model was configured with a 1/20° horizontal resolution, 40 terrain-following vertical levels, and 3 min time steps. The model employed a third-order upstream-rotated advection scheme, third-order upstream advection of momentum, and

50 the nonlocal K-profile (Large et al., 1994) closure scheme for vertical turbulent mixing. The initial temperature and salinity profiles used by the model were derived from the GLORYS (Global Ocean Reanalysis) Project (Lellouche et al., 2013). Our model was forced with monthly momentum means obtained from the GLORYS Project (Lellouche et al., 2013), monthly climatologies of heat and salt fluxes from the Comprehensive Ocean Atmosphere Data Set (da Silva et al., 1994), and 6 h wind

stress derived from the National Centers for Environmental Prediction (NCEP) Climate Forecast System Reanalysis (CFSR; Saha et al. (2010)) for 1998–2010 and the NCEP Climate Forecast System v. 2 (CFSv2; Saha et al. (2011)) for 2011–2013.

2.2 Biogeochemical model

The physical model was coupled with a biogeochemical model (Powell et al., 2006), which solves the nitrogen cycle using seven state variables [i.e., nitrate (NO3); ammonium (NH4); phytoplankton (Phy); chlorophyll (Chl); zooplankton (Zoo); and two groups of detritus, namely large (LDet) and small particles (SDet)]. In the biogeochemical model, a biological boundary condition was implemented in the bottom that was similar to the one proposed by Fennel et al. (2006). The boundary condition resolves the transformation process of organic matter that reaches the bottom, which was composed of detritus and phytoplankton in this case. This organic matter is instantly remineralized into ammonium. The mathematical expression that defines this process is shown in Eq. (1):

$$\frac{\partial}{\partial t} NH4 \bigg|_{z=H} = (Phy|_{z=H} + SDet|_{z=H} + LDet|_{z=H}) \tag{1}$$

where $Phy|_{z=H}$, $SDet|_{z=H}$ and $LDet|_{z=H}$ are the amounts of phytoplankton, small detritus, and large detritus in the bottom layer, respectively. In finite differences, as implemented in the numerical model, this becomes:

$$\frac{NH4^t_{i,j,k=H} - NH4^{t-1}_{i,j,k=H}}{\Delta t} = Phy^k_{i,j,k=H} + SDet^k_{i,j,k=H} + LDet^k_{i,j,k=H} \tag{2}$$

In the model, 24 major rivers, including their discharge, water temperature, and nitrate and ammonia concentrations (Fig. 2 and 3) were implemented as daily freshwater inputs (13 in Mexico and 11 in the United States) using the data simulated by González-Ramírez and Parés-Sierra (2019) for the Mexican rivers of Usumacinta, Grijalva, Tonala, Papaloapan, Coatzacoalcos, and Panuco and from data measured by the US Army Corps of Engineers at Tabert Landing and Simmesport for the Mississippi River and Atchafalaya River, respectively. For the Brazos and the Rio Grande rivers, annual daily climatologies were calculated from the available data periods. These data were retrieved from the United States Geological Survey (USGS). For the initial and biological boundary conditions, NO3 and NH4 data from the World Ocean Atlas (Boyer et al., 2013) were used.

3 Results

A 21 year simulation (1993–2013) was conducted during which the model managed to satisfactorily reproduce the main hydrodynamic characteristics of the GoM. In particular, a Loop Current penetration at 27° N, the coherent release of anticyclonic

eddies from the Loop current, cyclonic circulation in the BOC region, inversion of the coastal current over the western shelf of the GoM, and two confluence areas (one over the US-Mexico border and another between the states of Veracruz and Tabasco) were observed. It was possible to acceptably reproduce the general processes involved in the dynamics of primary production

85   in the GoM. An annual cycle dominated by the wind, high nutrient concentrations in the coastal regions and in cyclonic eddies (primarily in the eddy of the BOC region), and lower nutrient concentrations in the Loop Current and anticyclonic eddies were identified (Fig. 4).

3.1   Surface chlorophyll concentration

In winter, the coupled model simulated the response of phytoplankton to erosion processes operating in the upper portion of

90   the nutrient layer due to intense vertical mixing related to atmospheric forcing (e.g., cold fronts from the pole entering the gulf). In spring, two processes occur: a decrease in the surface chlorophyll concentration associated with a reduction in wind intensity and increases in chlorophyll concentrations over the different regions of the continental shelf (i.e., LATEX, TAVE, and BOC). The increase in chlorophyll over these platforms was mainly associated with two factors, namely the change in the direction of the upwelling-favorable wind component and an accumulation of terrestrial nutrients transported by rivers, which

95   was primarily observed over the LATEX platform. In this region, nutrient inputs, which are mostly supplied by the Mississippi and Atchafalaya Rivers, occur during late winter and early spring (Walsh et al., 1989; Turner and Rabalais, 1999).

This process continues during the summer, and a minimum concentration of chlorophyll is observed at the surface due to water-column stratification. During autumn, this concentration gradually increases until the aforementioned winter conditions are once again observed. For the purposes of comparing observed and simulated concentrations of chlorophyll at the surface,

100   the gulf was divided into three large regions: the deep region (I), the southern coastal region (II), and the northern coastal region (III; Fig. 1). Region III was delimited at the mouth of the Rio Grande. In regions I and II, relatively strong correlations were observed between the monthly averages of the coupled model and those obtained from satellite images. In contrast, a relatively low correlation was observed in region III for these variables. The simulated concentrations were similar to those reported by Xue et al. (2013), Gomez et al. (2018a), and Damien et al. (2018). The values obtained from the simulations are

105   consistent with those from previous studies on coupled models (i.e., Fennel et al. (2011), Xue et al. (2013), Gomez et al. (2018a) and Damien et al. (2018)) and with the observational data of Hidalgo-González and Alvarez-Borrego (2008) and Pasqueron de Fommervault et al. (2017). Average values of 0.02–0.6 $\mathrm{mg\,m}^3$ were observed in the deep region along with a high concentration of chlorophyll ($< 10\,\mathrm{mg\,m}^3$) in the Mississippi delta, which the model was able to mostly reproduce for the spring months.

3.2   Vertical chlorophyll distribution

In order to evaluate the performance of the model to correctly reproduce the vertical distribution of chlorophyll in the water column, daily sampling from 0–250 m depth was carried out at point P1 (Fig. 1) during the 21 year simulation. In winter, a uniform vertical distribution of chlorophyll was observed from the surface to the depth of the mixed layer, which was defined as the depth at which the difference in density with regard to the reference depth (in this case 10 m) was 0.03 $\mathrm{kg\,m}^{-3}$. In

summer, the subsurface maximum was located between 40–90 m on average, and a maximum concentration of ~ 0.6 mg m^{-3}
was observed (Fig. 6). Both results are consistent with the data of Pasqueron de Fommervault et al. (2017) derived from APEX
profilers, and data simulated by Damien et al. (2018) using a coupled model that was different to the one used in the present
study. In the vertical profile of the chlorophyll concentration, it was possible to locate the passage of anticyclonic eddies
released from the Loop Current. The most evident were those that occurred during 1995–1999, 2000–2002, 2004–2008, 2010,
and 2013. In the simulations, two types of eddies were identified. The first type was characterized by a lack of nutrients due
to a deepening of the isopycnals and a small amount of erosion in the superficial layer of the nutricline, which resulted in
a relatively small response of the phytoplankton in the euphotic layer. The second type, as observed in 1998 and 1999, was
characterized by a phytoplankton response within the eddy that was not limited to the edges where the isopycnals are closer to
the surface. Consequently, phytoplankton fertilization occurred upon nutrients reaching the euphotic layer.

3.3 BOC and TAVE averages

To carry out a more detailed analysis in the areas in which the new data from Mexican rivers were integrated, daily averages of
surface chlorophyll (Fig. 7, b) and the upwelling-favorable wind component (Fig. 7, a) were calculated in the areas correspond-
ing to the continental TAVE (Fig. 1, a) and BOC (Fig. 1, b) shelves. The daily averages of surface chlorophyll in both regions
were calculated with two configurations of the coupled model: with and without the implementation of the river component. In
the BOC, it was possible to observe a greater difference between both configurations. This difference was associated with the
volume that entered through the Grijalva and Usumacinta rivers, which presented the highest flows in the southern region of
the gulf. The average flow of the Grijalva-Usumacinta system was ~ 3600 m^3 s^{-1} with maximum values up to 10000 m^3 s^{-1}.
On the other hand, as previously mentioned, the spatial daily wind averages were calculated, taking into account the upwelling-
favorable component in each region, the meridional component (N–S) for the TAVE region, and the zonal component (W–E)
for the BOC. Finally, the nitrate signals that reached the corresponding areas in the BOC through the Grijalva-Usumacinta
system and all local rivers in the TAVE and were calculated.

3.4 Coherence

To better understand the time scales in which the different processes occur in the TAVE and BOC regions and the mechanisms
associated with them, the coherence between the surface chlorophyll concentration $[c(t)]$ and the upwelling-favorable wind
component $[w(t)]$ was calculated. For this, the following equation was used:

$$\gamma_{cw}^2 = \frac{|G_{cw}(f)|^2}{G_c(f)G_w(f)} \tag{3}$$

where $G_c(f)$ and $G_w(f)$ are the power spectral density functions of $c(t)$ and $w(t)$, respectively, and $G_{cw}(f)$ is the cross-
spectral density function between $c(t)$ and $w(t)$. Coherence values will always satisfy $0 \leq \gamma_{cw}^2 \leq 1$. The dominant signals in

both the TAVE and BOC regions were the annual ones in the coherence between chlorophyll and wind (Fig. 8) with values of $\gamma^2_{TAVE} = 0.95$ and $\gamma^2_{BOC} = 0.90$, respectively. In both the TAVE and BOC regions, a second important peak ($\gamma^2_{TAVE} = 0.85$ and $\gamma^2_{BOC} = 0.75$) was observed in the 180 day period. The dominance of the annual wind cycle in the dynamics of the analyzed regions could be identified from the coherence calculation. Such a cycle may be associated with annual upwelling-favorable

150 southerly winds during summer. This contrasts with what was observed in the deep region, in which the annual cycle of the response of surface chlorophyll was associated with intense vertical mixing mainly due to cold fronts in the winter months. The correlation peak observed in the 180 day period may be associated with extraordinary southerly winds during the cold months (October–March). Such winds stimulate a response in the concentration of surface chlorophyll by favoring upwelling due to Ekman transport.

155 ## 3.5 Empirical Orthogonal Funcions

From the data of the daily surface concentration of chlorophyll obtained from the model for the TAVE and BOC regions (Fig. 1, a and b), the first three modes of the empirical orthogonal functions (EOFs) were calculated for the period of 1998–2013. To compare the results of the model with the available observations, the same procedure was followed as with the monthly satellite images produced by the Moderate Resolution Imaging Spectroradiometer (MODIS) sensor for the period of 2003–2013. To

160 facilitate the comparison between the observed and simulated data, monthly averages were calculated using the daily outputs of the model. Subsequently, chlorophyll concentration anomalies were used to calculate the EOFs and their corresponding principal components. To identify and associate the variability peaks in the principal components with hydrological processes, anomalies of the monthly flows of the Mexican rivers in the TAVE and BOC regions were calculated. The same was done for the Mississippi River, as it has been shown that the freshwater signal reaches the TAVE region.

165 In the TAVE region (Fig. 9), the first mode yielded 56% and 52% of the variance for the simulated and observed data, respectively. This mode was mainly associated with two factors: the effect of rivers and variations in the chlorophyll concentration associated with atmospheric events. The latter was related with multiple processes, such as cold fronts (which induce vertical mixing) and extraordinary winds from the south (upwelling favorable winds). The peaks in extraordinary variability (Fig. 9, lower panel) associated with the extraordinary flow events of the local and Mississippi rivers could be observed in 1998

170 (model only), 2008 (model and observations), and 2011 (model and observations). Moreover, the variability peaks associated with extraordinary flows were only associated with local rivers in 2007 (model) and 2010 (model and observations). Finally, peaks associated with extraordinary flows of the Mississippi River were only observed in 2004 (model), 2009 (model and observations), 2012 (model and observations), and 2013 (observations).

For the BOC (Fig. 10), a response to the annual flow cycle of the relevant rivers of the Grijalva-Usumacinta system in the

175 region was observed. The first mode corresponded to the response of surface chlorophyll due to the effect of rivers and represented 40% and 43% of the variance for the modeled and observed data, respectively. Such peaks associated with extraordinary flow events in the Grijalva-Usumacinta system could be observed in the periods of 1998–2000, 2002, 2004, and 2010 in the model. On the other hand, the responses observed in 2005 and 2013 were present in both the model and observations and may have been associated with the passage of hurricanes Bret (June 2005) and Barry (June 2013).

4 Discussion

4.1 Deep region

The annual cycle of the deep region of the Gulf of Mexico analyzed in this study is consistent with the model data that has been reported by Fennel et al. (2011), Xue et al. (2013), Gomez et al. (2018b), and Damien et al. (2018), cruise data analyzed by Hidalgo-González and Alvarez-Borrego (2008), and profiler data analyzed by Pasqueron de Fommervault et al. (2017) for both the surface and water column. This annual cycle appears to be stable and consistent in all simulation years. This cycle responds mainly to intense vertical mixing caused by winds associated with cold fronts that occur during October–March, mesoscale processes that are mainly associated with the Loop Current, and the eddies that emerge from the Loop Current and eject filaments of chlorophyll-rich water to the central region of the Gulf of Mexico. Regarding the vertical distribution of chlorophyll, the model was able to coherently reproduce the concentration, depth, and migration period of the subsurface maximum at the analyzed point. The obtained results were compared with the results of Pasqueron de Fommervault et al. (2017) and Damien et al. (2018) and were found to be consistent, reflecting the stable behavior of the primary production processes at work in this region of the gulf. The most significant discrepancy between the observed and simulated data occurred in the northern zone of the Yucatan shelf. This discrepancy could be the product of the configuration of the physical model and the characteristics of the region.

4.2 TAVE shelf

In the Tamaulipas-Veracruz shelf, the model was able to represent primary production dynamics in a manner consistent with the data obtained from satellite images regarding the surface concentration of chlorophyll. In the simulations, it was possible to observe the annual cycle of primary production, in which low concentrations were present in the coastal zone during the cold months (October–March) and higher concentrations were present during warm months (April–September). In spring and summer, a higher concentration of chlorophyll was observed on the coast due to two main factors: northerly winds that favored upwelling due to Ekman transport and nutrient contributions from local rivers when they reached their maximum discharge rate. In autumn and winter, a relatively lower concentration of chlorophyll in the southern and central regions was observed due to the decreased flow of local rivers and the reversal of the wind direction (north to south), which impeded upwelling. In the northern region of TAVE, moderate to high concentrations of chlorophyll were still present due to the arrival of freshwater from the Mississippi River that was advected from the LATEX shelf during the autumn and winter months. Likewise, it was possible to observe anomalous events or years with extraordinary concentrations of surface chlorophyll, both in the model and in the observations, highlighting the consistency associated with the variability peaks. These events were associated with extraordinary flow events in local rivers and the Mississippi and Atchafalaya Rivers. In the years in which the variability peaks did not seem to respond to extraordinary flows, anomalous events (or out of season events) with regard to the direction and magnitude of the wind may have been responsible, such as *southerly winds* causing upwelling during the cold months (in the case of the positive variability peaks) and *northerly winds* causing downwelling during the warm months (in the case of negative variability peaks)

4.3 BOC shelf

Similarly to what was observed in the TAVE region, an annual cycle could be observed in BOC with high and low chlorophyll
215 concentrations in the warm (April–September) and cold months (October–March), respectively. It is important to mention that
a smaller difference in the surface concentration of chlorophyll between these two seasons was observed in the BOC compared
to that of the TAVE region. This discrepancy could be associated with the differences among the flows of the local rivers in the
TAVE and BOC regions. In the BOC, the Grijalva-Usumacinta system maintains a minimum flow that contrasts with that of
the local rivers in the TAVE region. This favors a considerable contribution of terrestrial nutrients to the BOC, which is also
220 present during the winter months.

5 Conclusions

In the deep region of the gulf, the concentration and distribution (both superficial and vertical) of chlorophyll was mainly
dominated by the annual wind cycle, which was associated with the formation of cold fronts. In the TAVE and BOC regions,
the variation in the chlorophyll concentration was dominated by the annual wind cycle and the nutrients provided by local
225 rivers, in addition to the contributions from the Mississippi River in the case of the TAVE region. The variability peaks were
associated with extraordinary flow events of local rivers in the TAVE and BOC regions and of the Mississippi River in the
TAVE region, in addition to extraordinary cold fronts that were observed during April and May, although primarily in the
TAVE region. The differences in the chlorophyll concentrations between the TAVE and BOC regions were associated with
three main factors: differences in the magnitude of the wind, the topography of each region, and differences in the amount of
230 terrestrial nutrients provided by rivers.

Author contributions. Conceptualization: JGR, APS; Data curation: JGR, APS, JCM; Formal analysis: JGR, APS; Funding acquisition:
APS; Investigation: JGR; Methodology: JGR, APS; Project administration: APS; Resources: APS; Software: JGR, APS; Supervision: APS;
Validation: JGR, APS; Visualization: JGR; Writing – original draft: JGR; Writing – review & editing: JGR, APS, JCM.

Competing interests. The authors declare no conflict of interest. The funders had no role in the design of the study; in the collection, analyses,
235 or interpretation of data; in the writing of the manuscript; or in the decision to publish the results.

Acknowledgements. This study was supported by the National Council of Science and Technology (CONACyT) [project CF-MG-20191030200716411-
1727972] and the Mexican Ministry of Energy Trust [project 201441]. This is a contribution of the Gulf of Mexico Research Consortium
(CIGoM). This study was conducted using E.U. Copernicus Marine Service Information.

References

Boyer, T. P., Antonov, J. I., Baranova, O. K., Coleman, C., Garcia, H. E., Grodsky, A., Johnson, D. R., Locarnini, R. A., Mishonov, A. V., O'Brien, T. D., et al.: World Ocean Database 2013., 2013.

CONAGUA, C. N. d. A.: Estadísticas del Agua en México, Gerencia de Aguas superficiales e Ingeniería de Ríos, 2014.

da Silva, A. M., Young, C. C., and Levitus, S.: Atlas of surface marine data 1994, Vol. 4: Anomalies of fresh water fluxes, NOAA Atlas, NESDIS, 9, 1994.

Damien, P., Pasqueron de Fommervault, O., Sheinbaum, J., Jouanno, J., Camacho-Ibar, V. F., and Duteil, O.: Partitioning of the open waters of the Gulf of Mexico based on the seasonal and interannual variability of chlorophyll concentration, Journal of Geophysical Research: Oceans, 123, 2592–2614, 2018.

Debreu, L., Marchesiello, P., Penven, P., and Cambon, G.: Two-way nesting in split-explicit ocean models: algorithms, implementation and validation, Ocean Modelling, 49, 1–21, 2012.

Elliott, B. A.: Anticyclonic rings in the Gulf of Mexico, Journal of Physical Oceanography, 12, 1292–1309, 1982.

Fennel, K., Wilkin, J., Levin, J., Moisan, J., O'Reilly, J., and Haidvogel, D.: Nitrogen cycling in the Middle Atlantic Bight: Results from a three-dimensional model and implications for the North Atlantic nitrogen budget, Global Biogeochemical Cycles, 20, 2006.

Fennel, K., Hetland, R., Feng, Y., and Dimarco, S.: A coupled physical-biological model of the Northern Gulf of Mexico shelf: Model description, validation and analysis of phytoplankton variability, Biogeosciences, 8, 1881–1899, https://doi.org/10.5194/bg-8-1881-2011, 2011.

Gomez, F. A., Lee, S.-K., Liu, Y., Hernandez Jr, F. J., Muller-Karger, F. E., and Lamkin, J. T.: Seasonal patterns in phytoplankton biomass across the northern and deep Gulf of Mexico: a numerical model study, Biogeosciences, 15, 3567, 2018a.

Gomez, F. A., Lee, S.-K., Liu, Y., Hernandez Jr, F. J., Muller-Karger, F. E., and Lamkin, J. T.: Seasonal patterns in phytoplankton biomass across the northern and deep Gulf of Mexico: a numerical model study, Biogeosciences, 15, 3567, 2018b.

González-Ramírez, J. and Parés-Sierra, A.: Streamflow modeling of five major rivers that flow into the Gulf of Mexico using SWAT, Atmósfera, 32, 261–272, 2019.

Hidalgo-González, R. and Alvarez-Borrego, S.: Water column structure and phytoplankton biomass profiles in the Gulf of Mexico, Ciencias Marinas, 34, 197–212, 2008.

Large, W. G., McWilliams, J. C., and Doney, S. C.: Oceanic vertical mixing: A review and a model with a nonlocal boundary layer parameterization, Reviews of Geophysics, 32, 363–403, 1994.

Lellouche, J.-M., Le Galloudec, O., Greiner, E., Garric, G., Regnier, C., Drevillon, M., Bourdallé-Badie, R., Bricaud, C., Drillet, Y., and Le Traon, P.-Y.: The Copernicus Marine Environment Monitoring Service global ocean 1/12 physical reanalysis GLORYS12V1: description and quality assessment, 20, 19 806, 2013.

Pasqueron de Fommervault, O., Perez-Brunius, P., Damien, P., Camacho-Ibar, V. F., and Sheinbaum, J.: Temporal variability of chlorophyll distribution in the Gulf of Mexico: bio-optical data from profiling floats, Biogeosciences, 14, 5647–5662, 2017.

Powell, T. M., Lewis, C. V., Curchitser, E. N., Haidvogel, D. B., Hermann, A. J., and Dobbins, E. L.: Results from a three-dimensional, nested biological-physical model of the California Current System and comparisons with statistics from satellite imagery, Journal of Geophysical Research: Oceans, 111, 2006.

Rivas Camargo, D. A.: Renovación del agua profunda en el Golfo de México - Tesis de doctorado en ciencias, CICESE, 2006.

Saha, S., Moorthi, S., Pan, H.-L., Wu, X., Wang, J., Nadiga, S., Tripp, P., Kistler, R., Woollen, J., Behringer, D., et al.: The NCEP climate forecast system reanalysis, Bulletin of the American Meteorological Society, 91, 1015–1058, 2010.

Saha, S., Moorthi, S., Wu, X., Wang, J., Nadiga, S., Tripp, P., Behringer, D., Hou, Y., Chuang, H.-y., Iredell, M., et al.: NCEP Climate Forecast System Version 2 (CFSv2) 6-hourly Products, Research Data Archive at the National Center for Atmospheric Research, Computational and Information Systems Laboratory, 2011.

Turner, R. and Rabalais, N.: Suspended particulate and dissolved nutrient loadings to Gulf of Mexico estuaries, Biogeochemistry of Gulf of Mexico Estuaries, pp. 89–107, 1999.

Vázquez De La Cerda, A. M., Reid, R. O., DiMarco, S. F., and Jochens, A. E.: Bay of Campeche Circulation: An Update, Circ. Gulf Mex. Obs. Model., pp. 279–293, https://doi.org/10.1029/161GM20, 2005.

Walsh, J. J., Dieterle, D. A., Meyers, M. B., and Müller-Karger, F. E.: Nitrogen exchange at the continental margin: A numerical study of the Gulf of Mexico, Progress in Oceanography, 23, 245–301, 1989.

Xue, Z., He, R., Fennel, K., Cai, W.-J., Lohrenz, S., and Hopkinson, C.: Modeling ocean circulation and biogeochemical variability in the Gulf of Mexico, Biogeosciences, 10, 7219–7234, 2013.

Zavala-Hidalgo, J., Morey, S. L., and Brien, J. J. O.: Seasonal circulation on the western shelf of the Gulf of Mexico using a high-resolution numerical model, 108, 1–19, https://doi.org/10.1029/2003JC001879, 2003.

Zavala-Hidalgo, J., Gallegos-García, A., Martínez-López, B., Morey, S. L., and O'Brien, J. J.: Seasonal upwelling on the Western and Southern Shelves of the Gulf of Mexico, Ocean Dyn., 56, 333–338, https://doi.org/10.1007/s10236-006-0072-3, 2006.
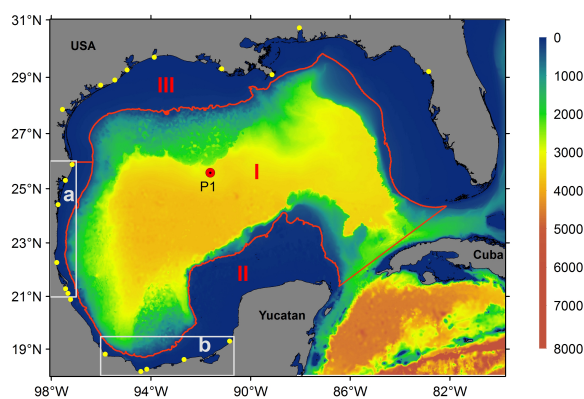
Figure 1. Gulf of Mexico bathymetry (m) and model domain. The yellow dots represent the rivers used in the model configuration. The red line represents the 200 m isobath that divides the gulf into three major regions: the deep region (I), southern coastal region (II), and northern coastal region (III). The gray areas were used to calculate daily chlorophyll, wind, and nitrate flux means in the Tamaulipas-Veracruz (TAVE; a) and Bay of Campeche (BOC; b) shelves, respectively.
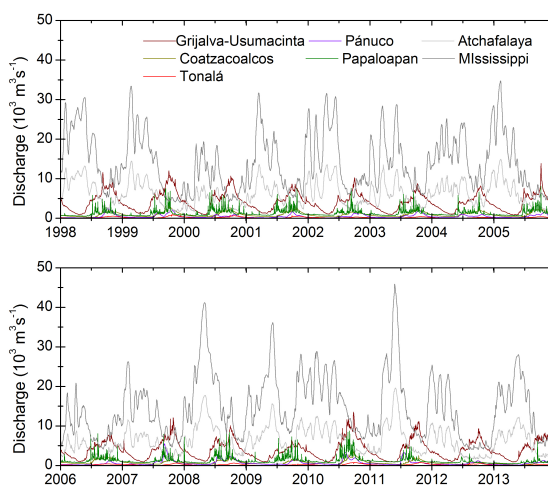
Figure 2. Observed (gray lines) and simulated (color lines) major river discharges used in the model. Seven out of 24 of the implemented rivers are shown.
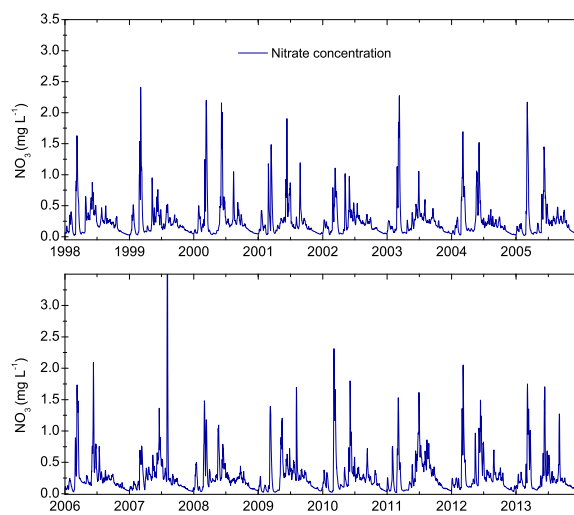
Figure 3. Nitrate concentrations in the Grijalva-Usimacinta river system from González-Ramírez and Parés-Sierra (2019) used in the model configuration.
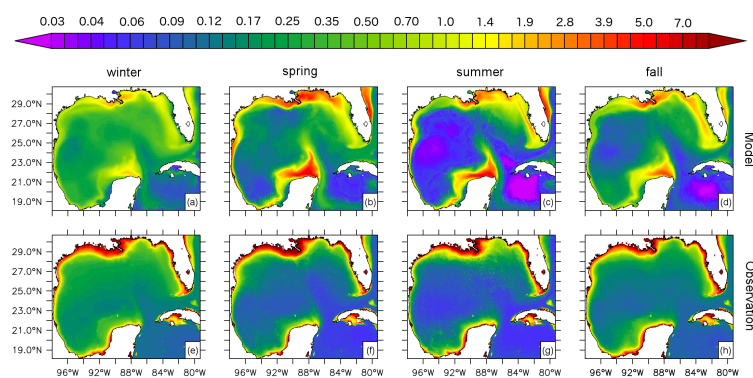
Figure 4. Seasonal climatologies of modeled and observed surface chlorophyll concentration in mg m^{-3}.
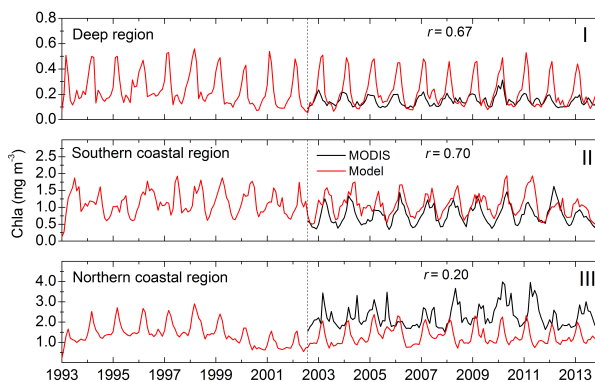
Figure 5. Monthly mean surface chlorophyll concentration. The black and red lines represent the observed and simulated data, respectively.
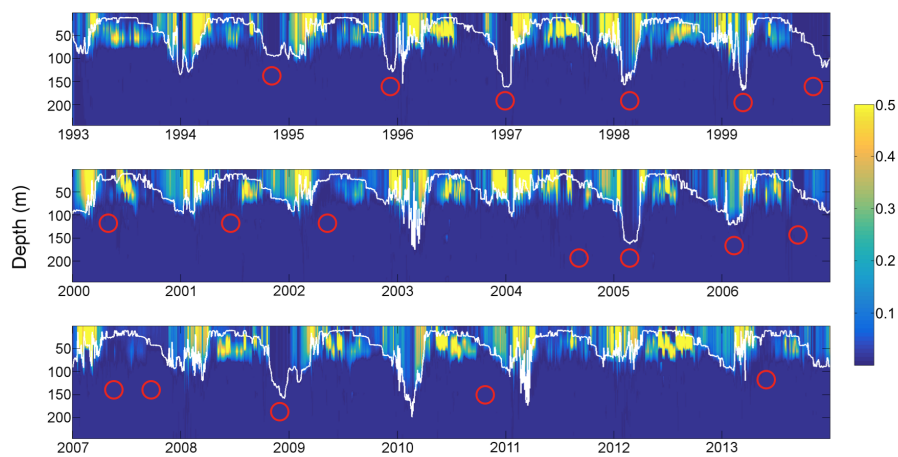
Figure 6. Daily chlorophyll concentration in $\mathrm{mg\ m^{-3}}$ sampled in P1. The mixed layer depth (MLD) is represented by the white line. The red circles show the passage of anticyclonic eddies through the point P1 during the simulation period.
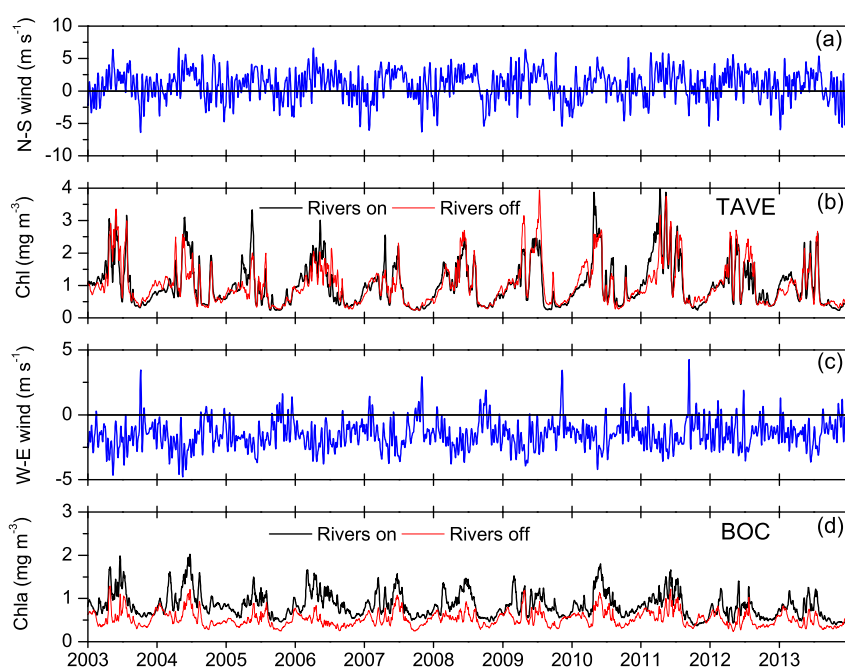
Figure 7. Panel (a) - Climate Forecast System Reanalysis (CFSR) 8-day, low-pass filtered N-S wind component for the Tamaulipas-Veracruz (TAVE) region. Positive values indicate upwelling favorable winds. (b) Average daily surface chlorophyll concentrations. (c) CFSR 8-day, low-pass filtered W-E wind component for the Bay of Campeche (BOC) region. Negative values indicate upwelling-favorable winds. (d) Average daily surface chlorophyll concentrations.
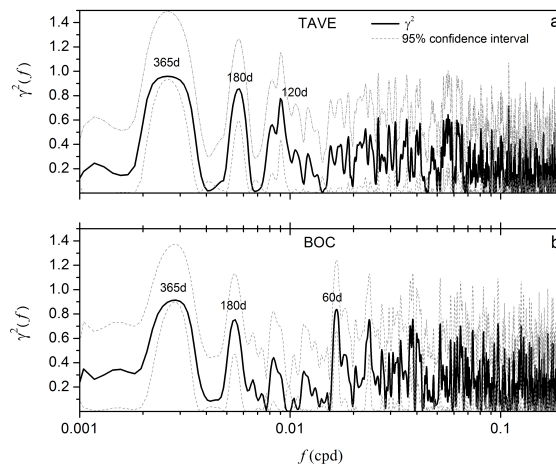
Figure 8. Coherence between daily surface chlorophyll concentration and upwelling favorable winds in the Tamaulipas-Veracruz (TAVE; a) and Bay of Campeche (BOC; b) regions.
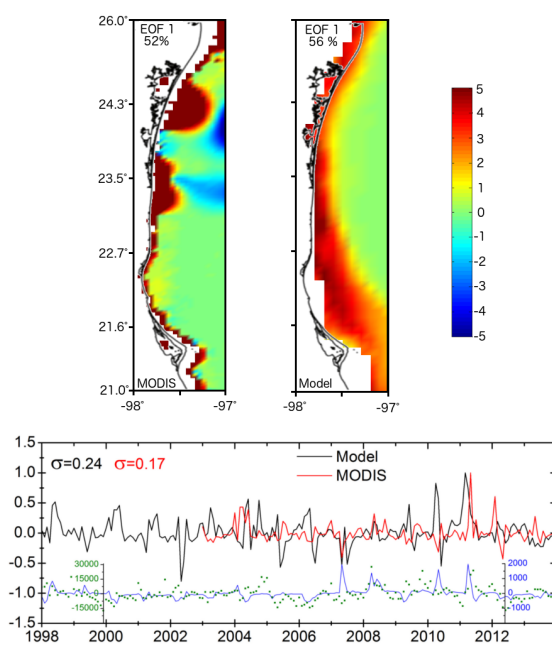
Figure 9. Top panel: Empirical orthogonal function (EOF) 1 calculated in Tamaulipas-Veracruz (TAVE) region from the model outputs (right) and monthly satellite imagery products (left). Lower panel: Principal component corresponding to mode 1 for the model outputs and observed data. The blue line shows the anomaly of the monthly net flow corresponding to all Mexican rivers that flow into the TAVE region. The green dots represent the anomaly of the monthly flow of the Mississippi River. All flows are given in $\mathrm{m^3 s^{-1}}$
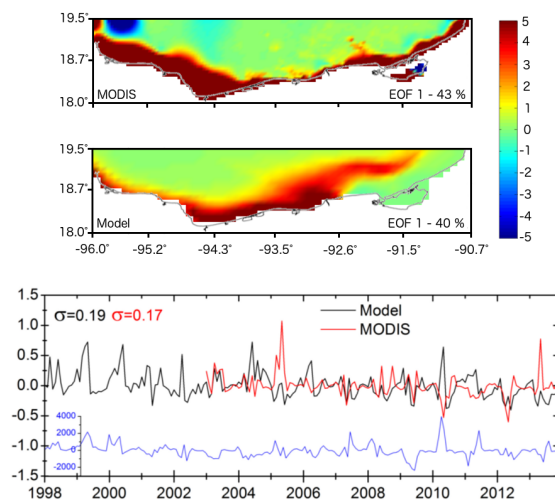
Figure 10. Top panel: Empirical orthogonal function (EOF) 1 calculated in the Bay of Campeche (BOC) region from the model outputs (right) and monthly satellite imagery products (left). Lower panel: Principal component corresponding to mode 1 for the model outputs and observed data. The blue line shows the anomaly of the monthly flow of the Grijalva-Usumacinta system in $\mathrm{m}^3\mathrm{s}^{-1}$
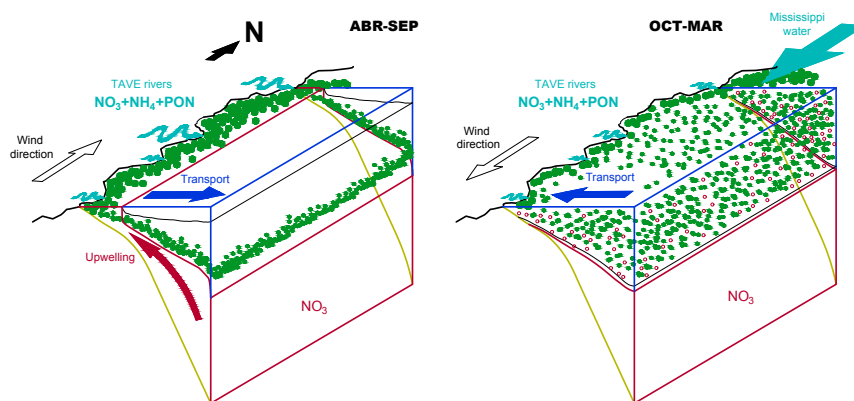
Figure 11. Primary production dynamics corresponding to spring and summer (right) and autumn and winter (left) on the Tamaulipas-Veracruz (TAVE) shelf. The green dots represent the chlorophyll concentration, and the red circles indicate the erosion of the nitrate reservoir due to a deepening of the mixed layer, which is represented by the black line
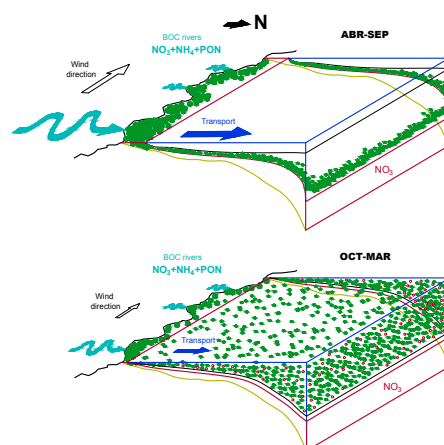
Figure 12. Primary production dynamics corresponding to spring and summer (top) and autumn and winter (bottom) on the BOC shelf. The green dots represent the chlorophyll concentration, the red circles the erosion of the nitrate reservoir due to the deepening of the mixed layer represented by the black line